Measured Versus Predicted High Temperature Langatate Behavior Up to 900°C

Peter Davulis and Mauricio Pereira da Cunha
Electrical and Computer Engineering Department
Laboratory for Surface Science and Technology
University of Maine, Orono, Maine, USA
email: mdacunha@eece.maine.edu

***Abstract*—This paper reports on surface acoustic wave (SAW) device measurements from room temperature to 900°C along six different orientations on langatate (LGT) wafers. The temperature behavior measured is compared to numerical predictions based on elastic constants extracted at high temperatures using resonant ultrasound spectroscopy techniques. SAW delay lines were fabricated on LGT wafers prepared at the University of Maine using 100 nm platinum-rhodium-zirconia electrodes capable of withstanding temperatures up to 1000°C. The frequency responses were used to extract the SAW velocities and temperature coefficients of delay. The results reported verify the existence of temperature compensated orientations at high temperature, which reinforce the interest in using LGT as a high temperature piezoelectric substrate.**

I. INTRODUCTION

The existence of piezoelectric materials capable of operating at high temperatures (>500°C) has generated the interest in a wide range of harsh environment and high temperature acoustic wave (AW) devices. Potential frequency control and sensing applications can be found in the aerospace, automotive, petroleum, energy, metallurgy, and manufacturing industries. Langatate (LGT), a crystal of the langasite family, is a promising high temperature AW substrate due to the absence of crystalline phase transitions up to its melting point (1470°C) and piezoelectric coefficients up to 3 times higher than quartz and 1.1 times higher than langasite [1]. In this paper we also experimentally identified the existence of temperature compensated orientations at elevated temperatures, adding this feature as an additional advantage for the use of LGT crystals.

In order to successfully design and implement high temperature AW devices, the crystal constants for acoustic wave propagation and design modeling need to be extracted at the corresponding elevated temperatures. In spite of high temperature characterization of LGT by some groups [2]-[5], a full set of LGT elastic constants and temperature coefficients above 200°C was only recently reported by the authors [6]. In that work, we used resonant ultrasound spectroscopy (RUS) measurements to extract the stiffened elastic constants from 25°C to 1100°C, and a second-order polynomial was employed to fit each elastic constant over the entire temperature range. The bulk and lattice expansion data used in this paper comes from previous measurements up to 1200°C made by the group and reported in [7].

In this paper, surface acoustic wave (SAW) delay line frequency measurements up to 900°C and along six selected LGT orientations are reported. The frequency measurements were used to extract the SAW phase velocity and the temperature coefficient of delay (TCD). These experimental results are compared to numerical predictions using the elastic constants and temperature coefficients reported in [6], thus permitting a first assessment of the previously reported constants and coefficients. SAW propagation was selected due to the possibility of fabricating multiple devices along diverse orientations out of a single wafer.

The LGT boules were X-ray aligned, cut, ground, and polished along rotated orientations at the University of Maine. SAW delay lines were fabricated on these wafers using 100 nm platinum-rhodium-zirconia ($Pt/Rh/ZrO_2$) electrodes capable of withstanding temperatures up to 1000°C [8].

Section II describes the process used to determine the selected crystal cut. Section III comments on the assumptions used to predict the SAW responses at high temperatures. Section IV details the device design, fabrication, and the measurement set-up. Section V compares measured and predicted frequency and TCD responses as a function of temperature and up to 900°C. Section VI concludes the paper.

II. DETERMINATION OF THE CRYSTAL CUT

In this work we targeted the selection of a crystal cut with the following properties: (i) singly rotated or having a first rotation aligned along major axes; (ii) relatively high SAW piezoelectric coupling (>0.2%) over most of the plane to allow the practical excitation of SAW along diverse orientations using the same wafer; (iii) significant variation of TCD around

Funding was provided in part by Petroleum Research Fund Grant ACS PRF# 42747-AC10, National Science Foundation Grant # ECS 0134335, and Air Force Office AFO Grants # FA9550-07-1-0519 and # F33615-03-D-5204.

the plane to allow for the verification of the predicted temperature coefficients using the constants previously reported in [6].

The cut identified which observed the previously mentioned conditions was Euler angles (φ, θ, ψ) = (90°, 23°, ψ). This particular cut offers interesting characteristics, namely: coupling K^2 >02% for most of the plane; a range of different TCD values at room temperature; and existence of temperature compensated orientations around room temperature with phase velocities >2700 m/s; and reduced diffraction (around -1) [9]. For this study six orientations with K^2 >02% were chosen on the (90°, 23°, ψ) cut, namely ψ=0°, ψ=13°, ψ=48°, ψ=77°, ψ=119°, and ψ=123°.

III. Predicted SAW Propagation Properties

The SAW phase velocity, frequency and TCD responses as a function of temperature were calculated from room temperature to 1100°C in increments of 10°C utilizing the constants and stiffened elastic temperature coefficients reported in [6]. In this work, the piezoelectric constants from [6] and dielectric constants from [10] were used. The temperature variations of the piezoelectric and dielectric constants were ignored, based on the assumption that their contribution to the SAW velocity is small when compared to the temperature variation of the elastic coefficients, as discussed in [6].

The uncertainty in the predictions was calculated using the reported uncertainties of the constants and temperature coefficients [6] using the method discussed in [9]. The uncertainties of these predicted SAW propagation properties were calculated at room temperature and used for the entire temperature range.

IV. Device Fabrication and Experimental Set-Up

SAW delay lines were designed and fabricated along (90°, 23°, ψ), ψ=[0°, 13°, 48°, 77°, 119°, 123°], orientations, including compensation for the power flow angle (PFA) for each respective orientation. Split-finger interdigitated transducers (IDTs) were used, with the fingers being 4μm wide, having 500 electrodes and a free region path of approximately 10.7 mm. The IDTs used apertures equal to 2.56 mm and 4.21 mm for the two IDTs in the delay line (about 80 and 130 wavelengths) to account for possible uncertainties in the PFA calculations and to accommodate variations of the PFA within the large temperature range.

LGT wafers were fabricated at the University of Maine (UMaine) Microwave Acoustic Material Laboratory using boules purchased from Fomos (Fomos-Materials, Moscow, Russia). The samples were aligned with a PANalytical X'Pert Pro MRD X-ray diffractometer (PANalytical Inc., Natick, Corp., Waltham, MA) to the plane (90°, 23°, ψ) using the process from [11] and [12], cut with an inner diameter saw (Meyer-Berger, Steffisberg, Switzerland), ground, and polished. The final polished finish had a RMS roughness of 6.7 Å and an average waviness of 95.9 Å, as measured by a surface profilometer. The SAW delay lines were fabricated using 105 to 108 nm thick co-deposited platinum-rhodium-zirconium-oxide ($Pt/Rh/ZrO_2$) electrodes [8]. These electrodes have been tested for long term operation up to 800°C and short term operation up to 1000°C [8]. In this work, we set the upper temperature limit to 900°C to avoid compromising the electrode quality. In fact, after repeated cycles up to 900°C, no measurable permanent device degradation was observed. The size of the wafer was constrained by the co-deposition chamber. For this reason, two different SAW wafers were fabricated, one with delay lines along ψ=0°, ψ=48°, and ψ=123° (Fig. 1) and another along ψ=13°, ψ=77°, and ψ=119°. The delay lines were bonded to high-temperature coaxial lines using 1 and 4 mil Pt wire with an Unitek parallel gap welder (Miyachi Unitek, Monrovia, CA). The high temperature tests were performed in laboratory air at atmospheric pressure inside a Thermolyne furnace (Thermolyne, Dubuque, IA).

The transmission (S_{21}) responses of the delay lines were measured with an Agilent 8753ES network analyzer (Agilent Technologies, Santa Clara, CA). The delay line responses were time-gated by windowing the inverse Fourier transform of the signal to remove the effect of electromagnetic feed through, SAW triple transit, and other acoustic spurious reflections. The SAW phase velocities were extracted from the measured center frequencies of the delay lines and the IDT periodicity corrected using the LGT thermal expansion coefficients from [7].

The TCD was calculated from the measurements using the relation

$$TCD = -TCF = -\left(\partial F \big/ \partial T\right) \big/ F \quad , \qquad (1)$$

where TCF is the temperature coefficient of frequency, F is the frequency, T is the temperature. For the high temperature furnace used in this study, small temperature steps were not feasible given the targeted large temperature range and the time it takes for the oven to reach an equilibrium temperature. The adopted temperature step in this work was Δt=50°C, and the frequency data points were obtained at least twice along

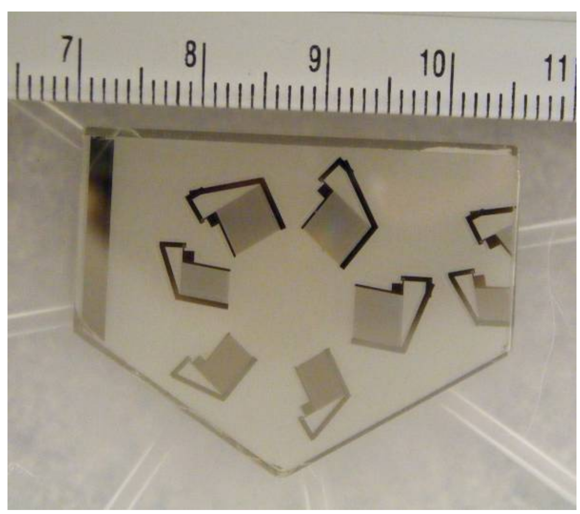

Figure 1. LGT wafer with delay line devices on the orientations (90°, 23°, ψ) for ψ=0°,48°,123°. The units of the ruler are cm.

each orientation. Along orientations where 0 TCD was found, the temperature step was decreased to Δt=10°C in the vicinity of 0 TCD in order to improve the TCD calculation. To calculate the derivative of the frequency with respect to temperature, polynomial fitting was used, and the slope was extracted out of the fitted curve. A fourth-order polynomial was used to provide a good correlation over the large temperature range (25 to 900°C). The discrete difference TCD was also calculated and used to verify the TCD obtained from the curve fitting.

The uncertainty in the temperature was calculated by considering both the furnace fluctuations due to the limitations of the furnace controller and the thermocouple precision. The standard deviation of each factor was combined to calculate the uncertainty of the measured quantity using regular error propagation [13]. The uncertainty in the frequency, σ_f, was calculated by [13]

$$\sigma_f = \sqrt{\frac{\sum_{i=1}^{N}(f_i - f_i^P)^2}{(N - O_P - 1)}}, \qquad (2)$$

where N is the number of data points, f_i is the i^{th} measured frequency, f_i^P is the frequency calculated from the polynomial fitting at the i^{th} temperature data point, and O_P is the polynomial order. The uncertainty in the TCD was calculated using the uncertainties in the temperature and the frequency fitted data. These uncertainties are quantified in Section V.

V. Results and Discussion

The SAW velocity and TCD were extracted from S_{21} measurements between 25°C and 900°C along the orientations (90°, 23°, ψ), where ψ=[0°, 13°, 48°, 77°, 119°, 123°], using the methods described in the previous section.

Figures 2a and 2b plot $\Delta f/f_0=(f(T)-f_0)/f_0$, with f_0 is the normalizing frequency at room temperature. Error bars are included for both calculated and experimental data. The $\Delta f/f_0$

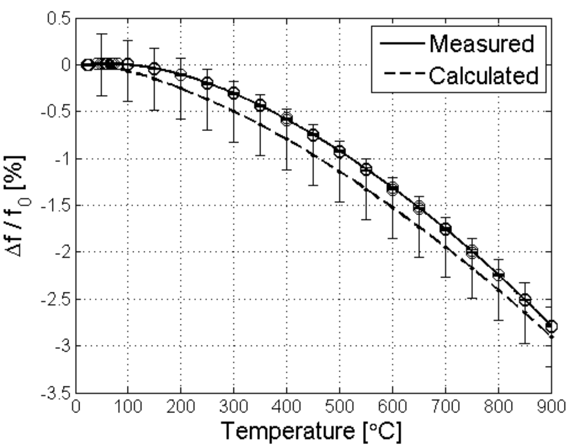

a) ψ=119°: Measured vs. predicted $\Delta f/f_0$

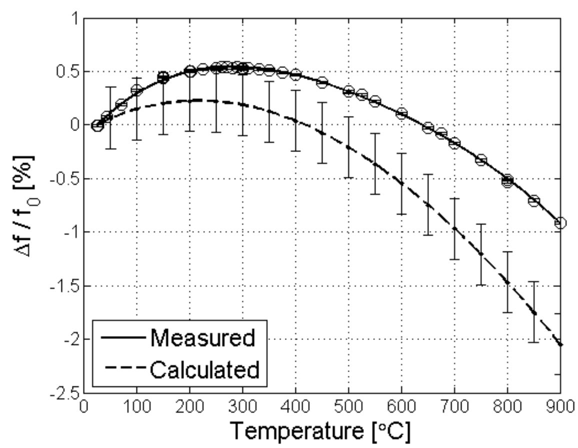

b) ψ=0°: Measured vs. predicted $\Delta f/f_0$

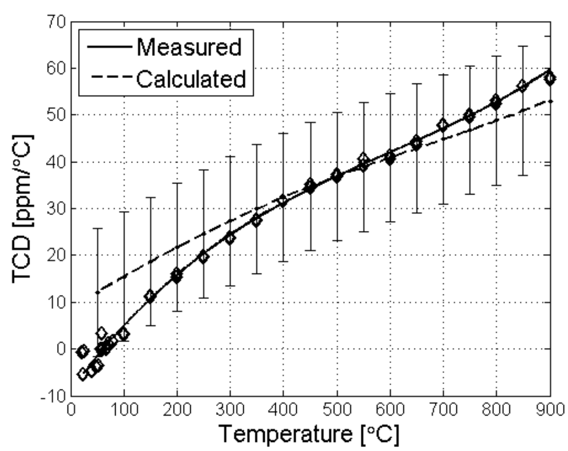

c) ψ=119°: Measured vs. predicted TCD

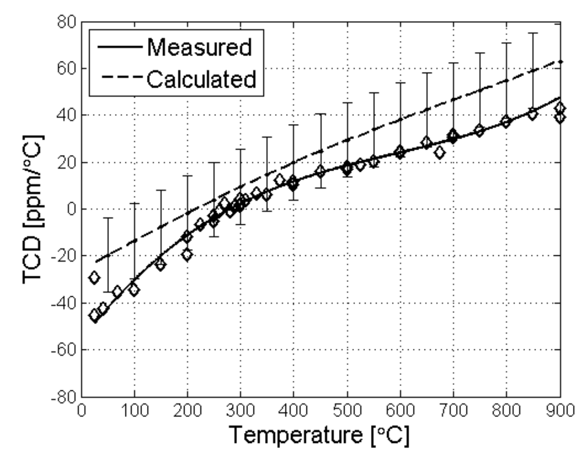

d) ψ=0°: Measured vs. predicted TCD

Figure 2. Example plots for measured and predicted $\Delta f/f_0$ and TCD. For all plots the solid curves are the measured data and the dashed curves are the predicted behavior. The circles on the $\Delta f/f_0$ plots (a and b) are the measured frequencies with error bars, which are difficult to see over the large temperature span. The diamonds on the TCD plots (c and d) are the values of TCD extracted by discrete differences, as described in Section IV.

curves for ψ=119° and ψ=0° were selected based on their turnover temperature: the first orientation has turnover temperature below 200°C, whereas the second, above 200°C. In fact out of the 6 orientations investigated, ψ=[119°, 123°] have a turnover temperatures below 100°C and the orientations ψ=[0°, 13°, 48°, 77°] have turnover temperatures above 200°C.

The uncertainty in the measured temperature ranges from 2.2°C around room temperature to 7°C or less at 900°C. The uncertainty in the frequency measurements is smaller than 18 kHz or 0.02%, which corresponds to an uncertainty of less than 0.55m/s or 0.02% in the measured velocity for all values of ψ over the entire temperature range. Using these numbers, the uncertainty in the TCD is less than 0.4 ppm/°C for all measured orientations over the entire temperature range.

The uncertainties in the predicted SAW phase velocity, frequency response, and TCD are larger than the uncertainties of these properties obtained through the measurements previously described. The uncertainties of the predicted SAW free surface velocities for the six orientations from 25°C to 900°C calculated as discussed in Section III are 0.2% or less than 6.3 m/s. The predicted TCD values have uncertainties ranging from 12 to 18 ppm/°C.

The difference between the measured and predicted SAW phase velocities and $\Delta f/f_0$ is less than 1.8% for all orientations investigated over the 25°C to 900°C temperature range. Along some orientations and at certain temperatures, the differences between the measured and predicted velocity and frequency responses are greater than the calculated uncertainties, as observed from Fig. 2b. Possible sources of such discrepancies are: (i) the assumption that the uncertainties in SAW phase velocity, frequency response, and TCD calculated at room temperature do not change with temperature. (ii) The use of the stiffened elastic constants to extract the temperature coefficients in [6]. (iii) The assumption the piezoelectric and dielectric constants can be treated as invariant with temperature. And finally, (iv) the presence of the IDTs, since the electrodes on top of a crystal will affect the measured temperature coefficients [14].

The measured and numerically predicted TCD for ψ=119° and ψ=0° are shown in Figs. 2c and 2d. The dashed lines are the TCD calculated using the constants in [6]. The solid line is the experimentally determined TCD, extracted by fitting a polynomial curve to the frequency data and using the slope to find the TCD, as described in the previous section. The diamonds are the discrete values of TCD computed directly from the differences between successive frequency measurements. The two methods of extracting the TCD from the experiments agree well, with the exception of end points of the measurement run.

The measured TCD curves for all the orientations investigated are plotted in Fig. 3. The TCD curves of ψ=13° and ψ=48° are almost identical and are close to that of ψ=77°.

The turnover temperatures (TCD=0) are of interest for the design of temperature compensated SAW devices. Table I compares the predicted and measured turnover temperature values for the SAW orientations investigated for which 0 TCD was measured. The discrepancies between the predicted and measured turnover temperature for the ψ=[0°, 13°, 48°, 77°] orientations are within 23%. Note that for ψ=119° and ψ=123° the turnover temperature is around room temperature, where the use of high temperature constants and coefficients from [6] are not as accurate as the temperature coefficients in [15] for the range from 25°C to 120°C. An investigation in the lower 25°C to 120°C temperature range is reported in [9] using the constants from [15].

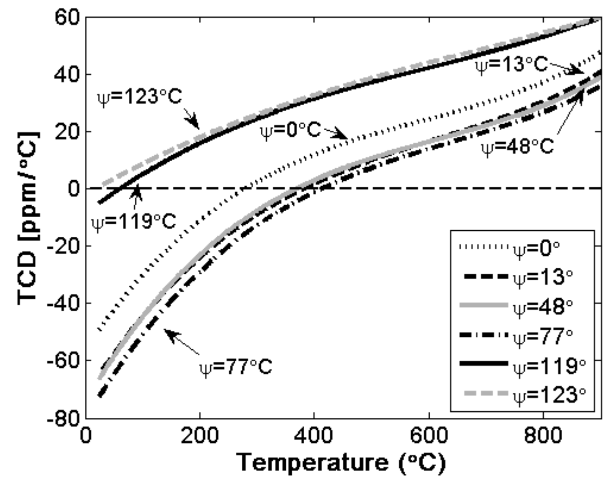

Figure 3. Measured TCD up to 900°C for the six measured orientations (90°, 23°, ψ), ψ=0° (dotted, black) , 13° (dashed, black), 48° (solid, gray), 77° (dot-dashed, black), 119° (solid, black), 123° (dashed, gray).

TABLE I. TURNOVER TEMPERATURES (TCD=0)

ψ (°)	Predicted (°C)	Measured (°C)
0	215	280
13	350	382
48	332	368
77	356	413
119	NA	62

VI. CONCLUSIONS

This work has reported on experimental LGT SAW delay line frequency response measurements from room temperature to 900°C using 6 different propagation directions. These measurements were compared to predicted SAW phase velocity, frequency, and TCD responses with temperature. The predicted behavior calculations were based on the LGT temperature coefficients measured between 25°C and 1100°C and previously reported by the authors. Overall, the measured and predicted responses agree reasonably well, and within less than 2% difference between measured and predicted SAW phase velocity and $\Delta f/f_0$ over the 25°C to 900°C temperature range.

This work predicted and verified the existence of 0 TCD orientations between 200 and 420°C for four of the orientation tested, i.e., along Euler angles (90°, 23°, ψ), ψ=[0°, 13°, 48°, 77°]. Along (90°, 23°, 119°) and (90°, 23°, 123°), the 0 TCD temperature was around 60°C. The predicted SAW piezoelectric coupling along ψ=[0°, 119°, 123°] are higher than 0.6% and along ψ=[13°, 48°, 77°] they are higher than 0.2%.

The results reported confirm the adequacy of the high temperature LGT elastic constants and temperature coefficients previously reported, which is important in identifying orientations and designing high temperature AW devices. In addition, the results reported in this work uncovered the existence of temperature compensated orientations at high temperature, reinforcing the interest in using LGT as a high temperature piezoelectric substrate.

REFERENCES

[1] J. A. Kosinski, "New piezoelectric substrates for SAW devices," Int'l J. of High Speed Electronics and Systems, vol. 10, no.4, 2000, pp 1017-1068.

[2] J. Schreuer, J. Rupp, C. Thybaut, and J. Stade, "Temperature dependence of elastic, piezoelectric, and dielectric properties of $La_3Ga_5SiO_{14}$ and $La_3Ga_{5.5}Ta_{0.5}O_{14}$: an application of resonant ultrasound spectroscopy," Proc. 2002 IEEE Ultrason. Symp., pp 373-376.

[3] J. Schreuer, C. Thybaut, M. Prestat, J. Stade, and E. Haussuhl, "Towards an understanding of the anomalous electromechanical behaviour of langasite and related compounds at high temperatures," Proc. 2003 IEEE Int'l Ultrason. Symp., pp 196-199.

[4] J. Schreuer, and C. Thybaut, "Anelastic relaxation effects and elastic instabilities in CGG-type compunds," Proc. 2005 IEEE Ultrason. Symp., pp 695-698.

[5] W. Johnson, S. Kim, and D. Lauria, "Anelastic loss in langatate," Proc. 2000 IEEE Int'l. Freq. Cont. Symp., pp 186-190.

[6] P. M. Davulis, A. Shyam, E. Lara-Curzio, M. Pereira da Cunha, "High temperature elastic constants of lLangatate from RUS measurements up to 1100°C," Proc. 2008 IEEE Int'l Ultrason. Symp., pp 2150-2153.

[7] T. R. Beaucage, E.P. Beenfeldt, S.A. Speakman, W.D. Porter, E.A. Payzant, M.Pereira da Cunha, "Comparison of high temperature crystal lattice and bulk thermal expansion measurements of LGT single crystal," Proc. 2006 IEEE Int'l Freq. Cont. Symp., pp 658-663.

[8] M. Pereira da Cunha, R. Lad, T. Moonlight, G. Bernhardt, D. Frankel, "High temperature stability of langasite surface acoustic wave devices," Proc. 2008 IEEE Int'l Ultrason. Symp., pp 205-208.

[9] B. Sturtevant, M. Pereira da Cunha, "Assessment of langatate material constants and temperature coefficients using SAW delay line measurements," Proc. 2009 IEEE Int'l Freq. Cntrl. Symp., in press.

[10] P. M. Davulis, B. T. Sturtevant, S. L. Duy, M. Pereira da Cunha, "Revisiting LGT dielectric constants and temperature coefficients up to 120 deg. C," Proc. 2007 Int'l Ultrason. Symp., pp 1397-1400.

[11] L. D. Doucette, M. Pereira da Cunha, R. J. Lad, "Precise orientation of single crystals by a simple X-ray diffraction rocking curve method," Rev. Sci. Instr., vol. 76, 036106, (4 pages), 2005.

[12] B. T. Sturtevant, M. Pereira da Cunha, R. J. Lad, "Determination of the absolute orientation of langatate crystals using X-ray diffraction," Proc. 2008 Int'l Ultrason. Symp., pp 741-744.

[13] J. R. Taylor, "An introduction to error analysis," 1st ed., Mill Valley, CA: University Science Books, 1982, pp153-172.

[14] M. Lewis, "Temperature compenstation techniques for SAW devices," Proc. 1979 IEEE Int'l Ultrason. Symp., pp 612-622.

[15] B. Sturtevant, P. Davulis, and M. Pereira da Cunha, "Pulse echo and combined resonance techniques: a full set of LGT acoustic wave constants and temperature coefficients," IEEE Trans. Ultrason., Ferroelect., Freq. Cont., vol. 56, no. 54, pp. 788-797, April 2009.